GDCh

Communications

Angewandte
Chemie
International Edition
www.angewandte.org

Discrete Stacked Dimers of Aromatic Oligoamide Helices

Daniel Bindl, Pradeep K. Mandal, Lars Allmendinger, and Ivan Huc*

Abstract: Tight binding was observed between the C-terminal cross section of aromatic oligoamide helices in aqueous solution, leading to the formation of discrete head-to-head dimers in slow exchange on the NMR timescale with the corresponding monomers. The nature and structure of the dimers was evidenced by 2D NOESY and DOSY spectroscopy, mass spectrometry and X-ray crystallography. The binding interface involves a large hydrophobic aromatic surface and hydrogen bonding. Dimerization requires that helices have the same handedness and the presence of a C-terminal carboxy function. The protonation state of the carboxy group plays a crucial role, resulting in pH dependence of the association. Dimerization is also influenced by neighboring side chains and can be programmed to selectively produce heteromeric aggregates.

Structurally precise and designable interaction interfaces are a key component of large self-assembled architectures. In this respect, folded molecules constitute building blocks of unmatched sophistication. The assemblies formed by proteins and nucleic acids in living systems, e.g. virus capsids or ribosomes, provide spectacular illustrations of the structures and functions enabled by assembling folded building blocks. There has thus been strong interest for programming interaction interfaces in artificial folded molecules. Great advances have been made using non-natural DNA[1] and protein[2] sequences. Using smaller molecules, the bundling of α-helical peptides is now so well understood that it permits reliable programming and function.[3] By extension, helix bundles have been produced from β-peptides[4] and urea-based γ-peptide isosteres.[5] Assemblies made of completely abiotic folded building blocks could bring advantages of their own including biochemical and thermal resistance as well as unrestricted functionalization. However, this line of research is less advanced because well-defined interaction interfaces have been lacking. Examples include the bundling of aromatic helices[6] and the formation of multistranded helices[7] and sheets[8] primarily in organic solvents. Here we report the serendipitous discovery of

stable discrete dimers of aromatic oligoamide helices in water. We find that aromatic stacking and hydrogen bonding mediate the dimerization of the helix C-terminal cross-section in a pH and side-chain-dependent manner. Aggregation can also be made heteromeric but, in all cases, it remains discrete. This contrasts with the stacking of many other aromatic objects,[9] including helices,[10] that tend to form polymeric assemblies.

Sequence **1** (Figure 1) comprises Q and B aromatic monomers that code for the formation of stable helices according to well-established design principles.[11] The chiral B^Rme unit was introduced to quantitatively bias handedness towards the *M* (left-handed) helix.[12] The various positively and negatively charged side chains provide solubility in water and were originally designed to promote helix bundling via side-chain mediated salt bridges. As shown in the following, helices do aggregate but not in the way initially intended.

[*] D. Bindl, Dr. P. K. Mandal, Dr. L. Allmendinger, Prof. I. Huc
Department of Pharmacy and Center for Integrated Protein Science
Ludwig-Maximilians-Universität
Butenandtstraße 5–13, München 81377 (Germany)
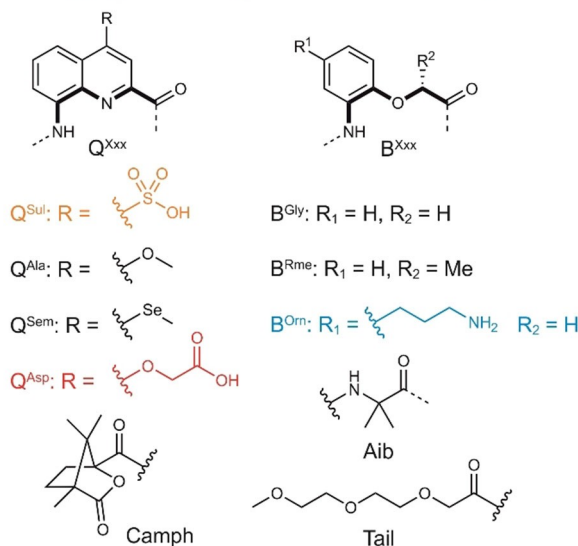E-mail: ivan.huc@cup.lmu.de

Figure 1. Sequences and building blocks that were investigated in this study. Monomers possessing charged side chains are highlighted with color (sulfonate: orange, carboxylate: red, ammonium: blue).

The ^{1}H NMR spectrum of **1** in water shows two sets of sharp signals the proportion of which change with concentration (Figure 2a), indicating a reversible aggregation phenomenon in slow exchange on the NMR timescale. The signals coalesce upon heating to 50°C (Figure S1). The number of signals indicate that the aggregate is on average symmetrical, i.e. its helical subcomponents are in the same environment. The signals of the aggregated species, including that of the CH_3 group of the B^{Rme} monomer below 0 ppm, are upfield-shifted. Upfield shifts associated with ring current effects are typically observed upon elongating helical sequences,[13] and suggest that helices of **1** may stack via their aromatic cross-section. The ESI-MS shows a large population of $[2M−2H]^{2−}$ and $[2M−3H]^{3−}$ dimeric species in the gas phase (Figure S2).

A crystal structure of **1** confirmed the expected helical structure (Figure 2b).[14] Packing in the lattice shows ex-
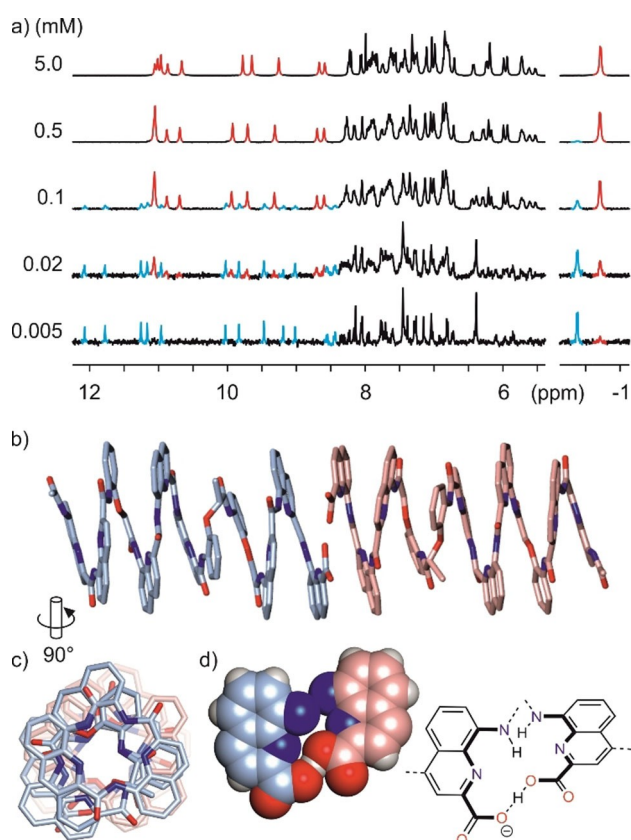
tended head-to-head stacks of helices and revealed several pairwise helix-helix contacts (Figure S23–S28). Rare intermolecular salt-bridges were dismissed as the possible driving force of aggregation in water. Stacking of the helix N-terminal cross sections involved a reduced aromatic surface and was also dismissed. In contrast aromatic contacts between the C-terminal cross sections were extensive (total buried surface of 431 Å²)[15] and accompanied by a close proximity of the terminal carboxy groups that can be attractive only if one of the two is in its protonated form (Figure 2d). In addition, tight side-by-side pair-wise contacts were observed that involve multiple hydrophobic aromatic and aliphatic CH groups that could not be dismissed without further experiment as the possible reason for aggregation in solution.

The ^{1}H NMR spectrum of the aggregate of **1** was assigned using bidimensional NMR experiments (Supporting Information section 3). NOE correlations were for most compatible with intramolecular contacts but at least two correlations could be explained only when the C-terminal cross-section of two helices are stacked (Figure 3a). In addition, analogous sequence **2**, which has the same side chains as **1** and a C-terminal Aib extension, does not aggregate and its signals are not upfield-shifted, i.e. they appear in the same range as those of the monomer of **1**. When mixed with **1**, compound **2** does not interfere with the aggregation of **1** and a DOSY spectrum shows that **2** is a smaller species despite having the additional Aib (Figure 3b), thus hinting at a monomeric state. In contrast shorter sequence **4** does aggregate in a similar manner as **1** (Figure S8).

Altogether, these data clearly support the formation of discrete dimers of **1** in aqueous solution via head-to-head stacking of the C-terminal cross-section. That simple stacking and one carboxyl-carboxylate hydrogen bond give rise to slow exchange on the NMR timescale is quite remarkable. Discrete aggregation mediated by aromatic stacking has been reported for some macrocycles[16] but it remains rare in aromatic systems which more frequently form polymeric aggregates. This discovery made us realize that several water-soluble aromatic helices that we have reported in the past presumably dimerize in the same way as they show the exact same stacking motif of the C-termini in the solid state.[17] This had however been overlooked.

The relative position of the carboxylate and carboxylic acid in the solid-state results in dissymmetry within the dimer (Figure 2d). In solution, NMR signals presumably reflect fast exchange between two degenerate dissymmetrical dimers upon proton exchange between the carboxylic acid and the carboxylate. The involvement of a carboxylic acid and a carboxylate was supported by different observations. Unlike sequence **4**, amide terminated analogous sequence **5** does not aggregate. In addition, the dimerization of **1** is hampered at higher pH (Figure S5). Dimerization at pH 7 in fact indicates a significantly increased apparent pK_a within the dimer. In the absence of external factors, the acid form is not expected at pH 7. These different effects explain why slightly different dissociation constants are calculated from the proportions of **1** and $(\mathbf{1})_2$ measured at different

Figure 2. a) ^{1}H NMR spectra of compound **1** at different concentrations in 27 mM sodium phosphate aqueous buffer pH 7.0. Selected distinct signals belonging to either the monomeric or dimeric form are highlighted in cyan and red, respectively. X-ray structure of **1** showing the stacking of two helices at their C-terminus in side view (b) and top view (c). The two crystallographically distinct molecules engaged in binding are colored in cyan and pink, respectively. Side chains, solvent molecules and hydrogen atoms are omitted for clarity. d) Fragment of the helix–helix binding interface showing the C-terminal monomers in space-filling representation. Side chains and solvent molecules are omitted. The acidic proton is not visible in the electron density map. The assignment of the carboxylic acid and carboxylate function is tentative, based on orientation.
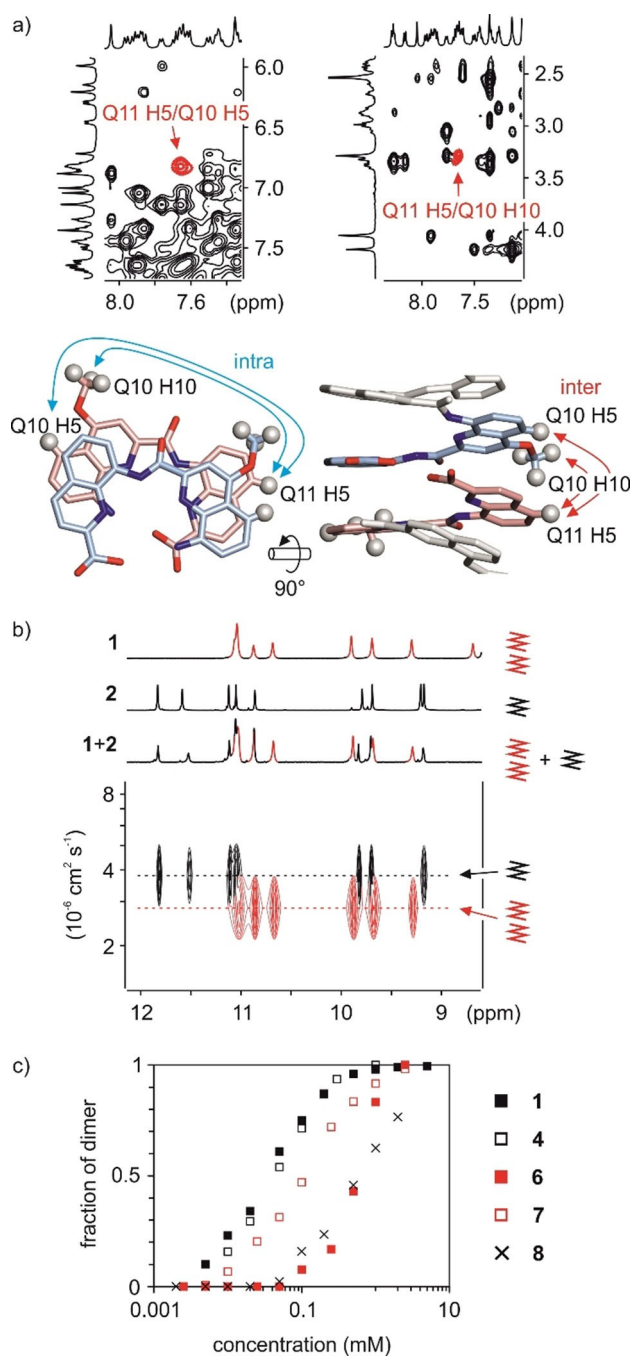
Figure 3. a) Selected parts of the NOESY spectrum of **1**. The intermolecular NOE correlations between Q11 H5/Q10 H5 and Q11 H5/Q10 H10 are highlighted in red. Structural models indicate the location of the protons involved in these correlations showing why these are likely to be intermolecular correlations and not intramolecular contacts. b) Amide-region of the ^{1}H NMR spectra of **1** (1 mM) in 27 mM sodium phosphate aqueous buffer pH 7.0, **2** (1 mM) and part of the DOSY spectrum of a mixture of **1** (1 mM) and **2** (1 mM) in 27 mM sodium phosphate aqueous buffer pH 7.0. Signals corresponding to compound **1** are highlighted in red. The two different levels of signals in the DOSY spectrum are indicated by dashed lines. c) ^{1}H NMR titration data of compounds **1**, **4**, **6–8** in 27 mM sodium phosphate aqueous buffer pH 7.0. Relative integrals of selected signals are plotted against sample concentration.

concentrations (Figure 2a): the extent of protonation also slightly depends on concentration and this impacts dimerization. Nevertheless, an average K_d value of 30 ±8 µmol can be extracted at neutral pH (27 mM phosphate buffer).

Dimerization was also investigated in sequences **6–8** (Figure 3c, S9–S11) and was found to vary by up to 20-fold from compound to compound. These results hint at possible intermolecular charge repulsions between side chain within the dimers and at possible effects of the electron richness of the quinoline rings at the helix-helix interface. For example, the difference between **6** and **7** is a simple change of position of a sulfonate. Based on the crystal structure of (**1**)$_2$, one can speculate about shorter intermolecular distances between anions in (**6**)$_2$ than in (**7**)$_2$ (Figure S12). From these results, one can envisage to tailor attractive interactions as well, e.g. intermolecular salt bridges between side chains.

In additional experiments, we explored the possibility to form heterodimers. We shall point again that each "homodimer" in fact consists of an acid and a carboxylate undergoing proton exchange. The "homodimer" is thus an average. Upon mixing (**1**)$_2$ and (**6**)$_2$ whose NMR signals differ due to the different lengths of **1** and **6**, a new species formed whose NMR chemical shift values suggest an intermediate length (Figure S13). This species could thus be reasonably assigned to heterodimer **1.6**. Depending on the sequences involved, the proportions between homo and heterodimers were found to vary as a reflection of their respective stability. Quantitative heterodimerization was achieved by mixing **1** and **5**. Sequence **5** cannot dimerize, but its primary amide can act as a hydrogen bond donor. Conversely, at higher pH, **1** is exclusively monomeric because its C-terminus is entirely deprotonated. Upon mixing the two, a single new species formed that was assigned to heterodimer **1.5** (Figure 4a).

Finally, we investigated stereochemical aspects of the dimerization. The crystal structure of (**1**)$_2$ (Figure 2b) and the presence of a single dimer in the NMR spectra of achiral sequences **3**, **6**, and **7** show that dimerization occurs between helices that have the same handedness and not between a P and an M helix. We reasoned that upon mixing an exclusively M dimer such as (**1**)$_2$ from chiral sequence **1** with a racemic P/M mixture of dimers such as (**3**)$_2$ from achiral sequence **3**, heterodimers **1.3** would form only with the M-helix of **3**. Heterodimerization would thus bias the handedness of **3** in favor of the M helix. Sequence **3** was therefore designed with additional flexibility (two pairs of contiguous B units) to allow for its helix handedness reversal to take place.[18,19] Circular dichroism spectra of mixtures of **1** and **3** in different proportions were recorded and demonstrated a deviation from linearity that perfectly matches with the predicted contribution of heterodimer **1.3**, assuming all three dimers have the same stability (Figure 4b, c, S14).

In summary we have characterized a binding interface between the C-terminal cross section of aromatic helices in water that is thermodynamically stable and undergoing slow exchange on the NMR timescale. Association is strictly dependent on the presence of a C-terminal main chain acid function and of helix handedness. In contrast, helix length likely has little influence. Association can be further tuned
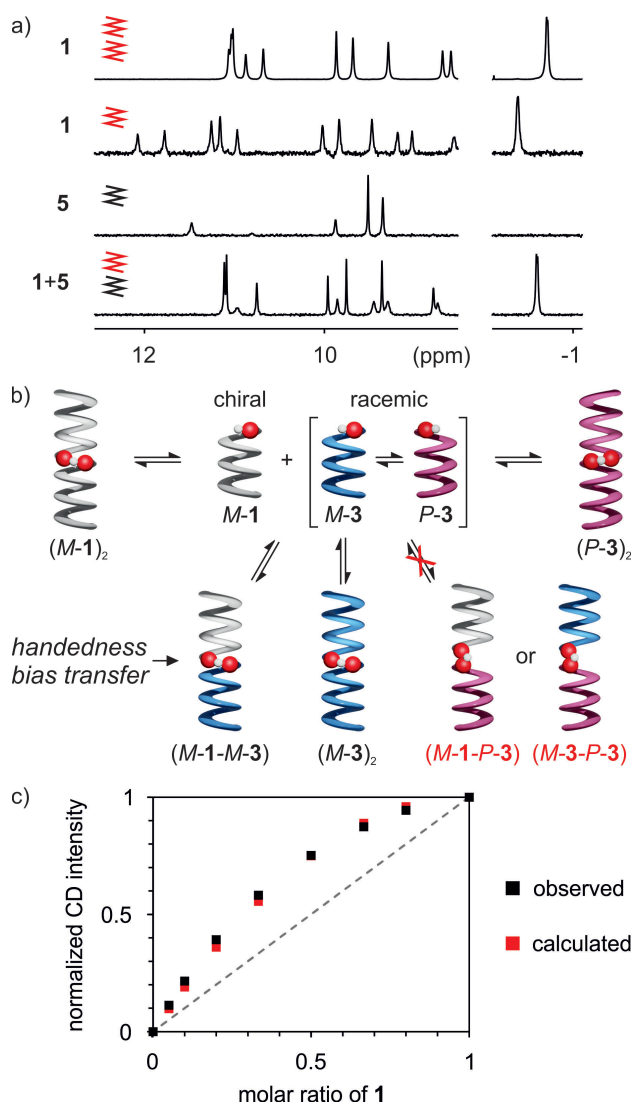
Figure 4. a) Parts of the ^{1}H NMR spectra of **1** (dimeric: 2 mM in 27 mM sodium phosphate aqueous buffer pH 7.0; monomeric: 0.1 mM in 12 mM ammonium acetate aqueous buffer pH 8.5), **5** (0.1 mM in 12 mM ammonium acetate aqueous buffer pH 8.5) and a mixture of **1** and **5** (0.1 mM and 0.1 mM in 12 mM ammonium acetate aqueous buffer pH 8.5). b) Scheme of equilibria present in a mixture of compounds **1** and **3**. C-termini are indicated by red and white spheres. Impossible aggregates are highlighted in red. c) Relative CD intensities of **1** mixed with **3** at different ratios (total $c = 0.5$ mM in water).

by charges borne by the helices and by pH. Selective heterodimerization can also be implemented. This interface may serve as a tool for the programmed assembly of various entities in water, including in combination with aromatic helix bundling, the initial and unmet objective of the work reported here, about which progress will be reported in due course.

Conflict of Interest

The authors declare no conflict of interest.

Data Availability Statement

The data that support the findings of this study are openly available in Cambridge Crystallographic Data Centre at https://ccdc.cam.ac.uk, reference number 2122518.

[1] a) L. L. Ong, N. Hanikel, O. K. Yaghi, C. Grun, M. T. Strauss, P. Bron, J. Lai-Kee-Him, F. Schueder, B. Wang, P. Wang, J. Y. Kishi, C. Myhrvold, A. Zhu, R. Jungmann, G. Bellot, Y. Ke, P. Yin, *Nature* **2017**, *552*, 72–77; b) K. F. Wagenbauer, C. Sigl, H. Dietz, *Nature* **2017**, *552*, 78–83.

[2] a) Y.-T. Lai, D. Cascio, T. O. Yeates, *Science* **2012**, *336*, 1129–1129; b) J. B. Bale, S. Gonen, Y. Liu, W. Sheffler, D. Ellis, C. Thomas, D. Cascio, T. O. Yeates, T. Gonen, N. P. King, D. Baker, *Science* **2016**, *353*, 389–394; c) Y. Hsia, J. B. Bale, S. Gonen, D. Shi, W. Sheffler, K. K. Fong, U. Nattermann, C. Xu, P.-S. Huang, R. Ravichandran, S. Yi, T. N. Davis, T. Gonen, N. P. King, D. Baker, *Nature* **2016**, *535*, 136–139; d) E. Golub, R. H. Subramanian, J. Esselborn, R. G. Alberstein, J. B. Bailey, J. A. Chiong, X. Yan, T. Booth, T. S. Baker, F. A. Tezcan, *Nature* **2020**, *578*, 172–176.

[3] a) A. J. Burton, A. R. Thomson, W. M. Dawson, R. L. Brady, D. N. Woolfson, *Nat. Chem.* **2016**, *8*, 837–844; b) T. Lebar, D. Lainšček, E. Merljak, J. Aupič, R. Jerala, *Nat. Chem. Biol.* **2020**, *16*, 513–519.

[4] a) D. S. Daniels, E. J. Petersson, J. X. Qiu, A. Schepartz, *J. Am. Chem. Soc.* **2007**, *129*, 1532–1533; b) W. C. Pomerantz, V. M. Yuwono, C. L. Pizzey, J. D. Hartgerink, N. L. Abbott, S. H. Gellman, *Angew. Chem. Int. Ed.* **2008**, *47*, 1241–1244; *Angew. Chem.* **2008**, *120*, 1261–1264.

[5] a) G. W. Collie, K. Pulka-Ziach, C. M. Lombardo, J. Fremaux, F. Rosu, M. Decossas, L. Mauran, O. Lambert, V. Gabelica, C. D. Mackereth, G. Guichard, *Nat. Chem.* **2015**, *7*, 871–878; b) C. M. Lombardo, G. W. Collie, K. Pulka-Ziach, F. Rosu, V. Gabelica, C. D. Mackereth, G. Guichard, *J. Am. Chem. Soc.* **2016**, *138*, 10522–10530; c) G. W. Collie, R. Bailly, K. Pulka-Ziach, C. M. Lombardo, L. Mauran, N. Taib-Maamar, J. Dessolin, C. D. Mackereth, G. Guichard, *J. Am. Chem. Soc.* **2017**, *139*, 6128–6137.

[6] a) S. De, B. Chi, T. Granier, T. Qi, V. Maurizot, I. Huc, *Nat. Chem.* **2018**, *10*, 51–57; b) D. Mazzier, S. De, B. Wicher, V.

Maurizot, I. Huc, *Chem. Sci.* **2019**, *10*, 6984–6991; c) D. Mazzier, S. De, B. Wicher, V. Maurizot, I. Huc, *Angew. Chem. Int. Ed.* **2020**, *59*, 1606–1610; *Angew. Chem.* **2020**, *132*, 1623–1627.

[7] a) J. Shang, Q. Gan, S. J. Dawson, F. Rosu, H. Jiang, Y. Ferrand, I. Huc, *Org. Lett.* **2014**, *16*, 4992–4995; b) B. Baptiste, J. Zhu, D. Haldar, B. Kauffmann, J.-M. Léger, I. Huc, *Chem. Asian J.* **2010**, *5*, 1364–1375; c) Y. Ferrand, A. M. Kendhale, J. Garric, B. Kauffmann, I. Huc, *Angew. Chem. Int. Ed.* **2010**, *49*, 1778–1781; *Angew. Chem.* **2010**, *122*, 1822–1825; d) Y. Tanaka, H. Katagiri, Y. Furusho, E. Yashima, *Angew. Chem. Int. Ed.* **2005**, *44*, 3867–3870; *Angew. Chem.* **2005**, *117*, 3935–3938; e) H. Goto, H. Katagiri, Y. Furusho, E. Yashima, *J. Am. Chem. Soc.* **2006**, *128*, 7176–7178; f) E. Yashima, N. Ousaka, D. Taura, K. Shimomura, T. Ikai, K. Maeda, *Chem. Rev.* **2016**, *116*, 13752–13990.

[8] a) J. Zhu, J.-B. Lin, Y.-X. Xu, X.-B. Shao, X.-K. Jiang, Z.-T. Li, *J. Am. Chem. Soc.* **2006**, *128*, 12307–12313; b) B. Gong, Y. Yan, H. Zeng, E. Skrzypczak-Jankunn, Y. W. Kim, J. Zhu, H. Ickes, *J. Am. Chem. Soc.* **1999**, *121*, 5607–5608; c) X. Yang, S. Martinovic, R. D. Smith, B. Gong, *J. Am. Chem. Soc.* **2003**, *125*, 9932–9933; d) B. Gong, *Acc. Chem. Res.* **2012**, *45*, 2077–2087; e) J. Atcher, P. Mateus, B. Kauffmann, F. Rosu, V. Maurizot, I. Huc, *Angew. Chem. Int. Ed.* **2021**, *60*, 2574–2577; *Angew. Chem.* **2021**, *133*, 2605–2609; f) E. A. Archer, A. E. Sochia, M. J. Krische, *Chem. Eur. J.* **2001**, *7*, 2059–2066; g) E. A. Archer, M. J. Krische, *J. Am. Chem. Soc.* **2002**, *124*, 5074–5083; h) H. Gong, M. J. Krische, *J. Am. Chem. Soc.* **2005**, *127*, 1719–1725.

[9] a) J. W. Sadownik, E. Mattia, P. Nowak, S. Otto, *Nat. Chem.* **2016**, *8*, 264–269; b) X. Zhou, G. Liu, K. Yamato, Y. Shen, R. Cheng, X. Wei, W. Bai, Y. Gao, H. Li, Y. Liu, F. Liu, D. M. Czajkowsky, J. Wang, M. J. Dabney, Z. Cai, J. Hu, F. V. Bright, L. He, X. C. Zeng, Z. Shao, B. Gong, *Nat. Commun.* **2012**, *3*, 949.

[10] a) Y. Huo, H. Zeng, *Acc. Chem. Res.* **2016**, *49*, 922–930; b) H. Zhao, S. Sheng, Y. Hong, H. Zeng, *J. Am. Chem. Soc.* **2014**, *136*, 14270–14276; c) H. Zhao, W. Q. Ong, F. Zhou, X. Fang, X. Chen, S. F. Y. Li, H. Su, N.-J. Cho, H. Zeng, *Chem. Sci.* **2012**, *3*, 2042; d) J. Shen, R. Ye, A. Romanies, A. Roy, F. Chen, C. L. Ren, Z. Liu, H. Zeng, *J. Am. Chem. Soc.* **2020**, *142*, 10050.

[11] a) I. Huc, *Eur. J. Org. Chem.* **2004**, 17–29; b) D.-W. Zhang, X. Zhao, J.-L. Hou, Z.-T. Li, *Chem. Rev.* **2012**, *112*, 5271–5316.

[12] D. Bindl, E. Heinemann, P. K. Mandal, I. Huc, *Chem. Commun.* **2021**, *57*, 5662–5665.

[13] N. Delsuc, T. Kawanami, J. Lefeuvre, A. Shundo, H. Ihara, M. Takafuji, I. Huc, *ChemPhysChem* **2008**, *9*, 1882–1890.

[14] Deposition Numbers 2122518 contain the supplementary crystallographic data for this paper. These data are provided free of charge by the joint Cambridge Crystallographic Data Centre and Fachinformationszentrum Karlsruhe Access Structures service.

[15] Solvent accessible surface of two monomers minus the solvent accessible suface of one dimer, as calculated in PyMOL Molecular Graphics System, Version 1.2r3pre, Schrödinger, LLC.

[16] a) L. Shu, M. Mayor, *Chem. Commun.* **2006**, 4134; b) X. Wu, R. Liu, B. Sathyamoorthy, K. Yamato, G. Liang, L. Shen, S. Ma, D. K. Sukumaran, T. Szyperski, W. Fang, L. He, X. Chen, B. Gong, *J. Am. Chem. Soc.* **2015**, *137*, 5879.

[17] X. Hu, S. J. Dawson, P. K. Mandal, X. De Hatten, B. Baptiste, I. Huc, *Chem. Sci.* **2017**, *8*, 3741–3749.

[18] M. Vallade, P. Sai Reddy, L. Fischer, I. Huc, *Eur. J. Org. Chem.* **2018**, 5489–5498.

[19] Handedness reversal of long helices can be kinetically blocked in water, unless some more flexible units are introduced.